PS-b-PEO Diblock Copolymer Selectively Dispersed with CdS Quantum Dots

The study is to investigate on the interaction between the block copolymer and nanoparticles on the effect of nanoparticles in the morphology of block copolymers. Work has been done in preparation of self-assembled CdS/PS-b-PEO nanocomposites and observation on selective distribution of CdS nanoparticles in the PEO block of diblock copolymers and the resulting morphological changes. Particular interest was set on the phenomena such that CdS nanoparticles induced the PEO domains to change from hexagonally-packed PEO cylinders to body-centered cubic or simple cubic CdS/PEO spheres

Block copolymers are versatile platform materials because they can self-assemble into various nanostructures with period thicknesses between 10 to 100 nm under the appropriate compositions and conditions, owing to microphase separation between incompatible blocks. In recent years, a number of studies of involving applications of nanostructured block copolymer as nano-template, nano-masks for lithography and photonic crystal have been reported. Specifically, the wok on nanometer-scale surface pattern with long range order created by crystallization of asymmetric PB-b-PEO by Reiter is an interesting one. In another case, sorting out different sizes of CdSe nanoparticles into PS-b-PMMA porous template with capillary force was carried out by Russell et al. Several group also reported the use of block copolymer as nanotemplates to grow Co, Ag, Au nanowires or to control the spatial locations of nanoparticles such as TiO_2 and Pd. Moreover, block copolymer lithography with large area nanoscale patterning by Register et al. has also been reported. These studies motivated us to investigate the interaction between the block copolymer and nanoparticles, particularly on the effect of nanoparticles in the morphology of block copolymers.

For semiconductor nanoparticles with sizes close to their Bohr exciton radius (typically between 1-10 nm), the size-dependent band gap results in tunable optical properties. These semiconductor nanoparticles are termed as quantum dots (QDs) because their tunable optical properties can be predicted by quantum mechanics. Nanoparticles that are not treated with a surfactant or bonded to polymer chains will, however, from large aggregates.

The use of nanostructured block copolymers as templates to selectively control the spatial location of semiconductor nanoparticles in one of the blocks may lead to several potential applications. For instance, periodic high refractive index contrast domains in phase-separated block copolymers can be used in photonic crystal applications. Nanoparticles with highly efficient luminescence can be combined with organic layers in light-emitting devices. The incorporation of nanoparticles into block copolymers, however, would lead to more complicated block copolymer morphologies than their pristine state as predicted by Balazs'group, which used a self-consistent field theory and a density functional theory for describing the polymer and the nanoparticles, respectively, to predict the morphology and phase diagram. In this article, we report the selective distribution of CdS QDs in the PEO block of a diblock copolymer, PS-b-PEO, and the resultant morphological changes. Specifically, CdS QDs induce the PEO domains to change from hexagonally-packed cylinders to body-centered cubic or simple cubic spheres, as shown in Scheme 1. To our knowledge, this is the first study concerning the morphological transformation of block copolymer by nanoparticles.

For the present study, an asymmetric polystyrene-b-poly (ethylene oxide) diblock copolymer (PS-b-PEO) with a molecular weight ratio of 125K

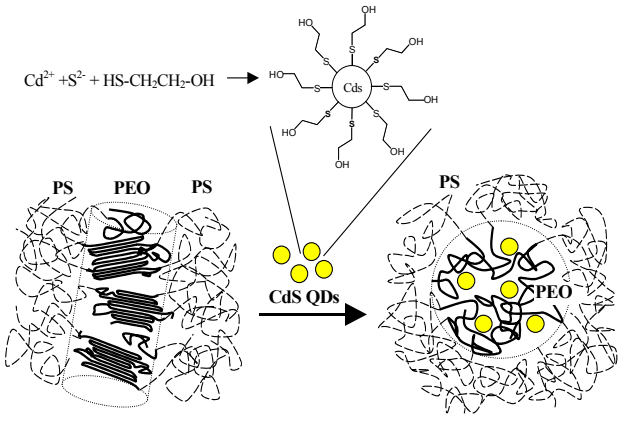

Scheme 1: Morphological transformation of PS-b-PEO diblock copolymer by selectively dispersed colloidal CdS QDs.

Table 1: Characteristic Properties of CdS nanoparticles

Absorption onset (λo)[a]	Particle size in DMF[b]	Emission wavelength[c]	Crystal size[d]	Average particle size[e]
447 nm	3.37 nm	650 nm	1.33 nm	2.5 nm

[a] The onset absorption wavelength of CdS nanoparticles in DMF as obtained from UV-vis spectra.

[b] The sizes of CdS nanoparticles in DMF were calculated with the onset absorption obtained by UV-Vis spectra using the following equation.

$$Eg_{os} - Eg_{ref} = \Delta Eg \approx \frac{\hbar^2\pi^2}{2R^2} \bullet \frac{1}{\mu} - \frac{1.8e^2}{\varepsilon R}$$

[c] The emission wavelength is determined from the photoluminescence.

[d] Crystal sizes are calculated using the Debye-Scherrer equation.

[e] The averaged size of CdS was obtained from SAXS curves of CdS/PS-b-PEO in Figure 1.

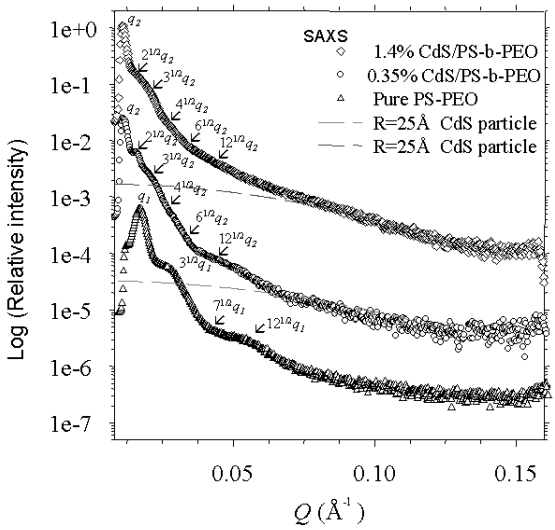

Fig. 1: *Synchrotron SAXS curves of PS-b-PEO and CdS/PS-b-PEO.*

/16.1K was purchased from Polymersource Inc. CdS nanoparticles were synthesized with mercaptoethanol as the surfactant. In our case, surfactant-modified CdS containing a chemically active hydroxyl surface, as shown in Scheme 1, become hydrophilic, and their basic properties are given in Table 1. Subsequently, CdS/DMF was added to a previously prepared PS-b-PEO/DMF solution under stirring. This mixture was dried and then annealed, and then the CdS/PS-b-PEO nanocomposite film was obtained.

Small-angle X-ray scattering experiments were performed on wiggler beamline 17B1 at NSRRC. Wide-angle X-ray diffraction on samples was collected by using a conventional rotating anode source. For transmission electron microscopy (TEM) and atomic force microscopy (AFM), the thin specimens were microtomed with Leica Ultracut Uct. TEM images were obtained with Hitachi H-600 transmission electron microscope. AFM measurements were performed in taping-mode with a Digital Nanoscope IIIa under ambient conditions. The glass transition temperatures (Tg) and melting point (Tm) were obtained from a Dupont DSC 2910 at a heating rate of 20℃/min. Photoluminescence spectra (PL) were obtained with a Hitachi F4500 fluorescence spectrophotometer at room temperature.

Figure 1 shows one-dimension small-angle X-ray scattering patterns (SAXS) of PS-b-PEO and CdS/PS-b-PEO nanocomposites by synchrotron radiation. For pure PS-b-PEO, four peaks appear at Q = 0.016, 0.027, 0.032 and 0.042 Å^{-1}, corresponding to a ratio of 1:$3^{1/2}$:$4^{1/2}$:$7^{1/2}$. This ratio indicates typical scattering by hexagonally-packed cylinders (HEX). The inter-cylinder distance (D) was determined to be 45.3 nm by equation (1).

$$D = \left(\frac{4}{3}\right)^{1/2} * d_{100} \quad (1)$$

where $d_{100}=2\pi/Q_{100}$ and Q_{100}= 0.16 nm^{-1}. In the case of PS-b-PEO containing 0.35% CdS, the scattering peaks are located at Q = 0.0114, 0.0158, 0.0203, 0.0228, 0.0281 and 0.0399 Å^{-1}, which gives a ratio of 1: $2^{1/2}$:$3^{1/2}$:$4^{1/2}$:$6^{1/2}$:$12^{1/2}$. This ratio implies that the scattering is caused by either body-centered cubic packed spheres (BCC) or simple cubic spheres (SC). The inter-sphere distance is 67.5 nm, as determined from equation (2).

$$D = \left(\frac{3}{2}\right)^{1/2} * d_{110} \quad (2)$$

where $d_{110}=2\pi/Q_{110}$ and Q_{110}= 0.114 nm^{-1}. SAXS results confirm that the nanostructured HEX structure of pure PS-b-PEO has been transformed to a BCC or SC morphology, due to the presence of CdS QDs. The size of CdS QDs in the block copolymer is about 2.5 nm, as derived from the structure form of the SAXS curve.

Figure 2(a) and (b) show the transmission electron microscopy (TEM) images of PS-b-PEO stained with OsO_4 and CdS/PS-b-PEO without staining, respectively. PEO domains appear in dark phase in Figure 2(a), owing to selective staining, and display as short cylinders. In the case of CdS/PS-b-PEO, however, periodic dark spherical phases of CdS-included PEO appear, and no pure PEO domains without CdS QDs could be observed. The location of CdS in the PEO domain is revealed by energy dispersive spectrometry. Dark phases are caused by the higher electron density of cadmium relative to that of PS-b-PEO. The selective

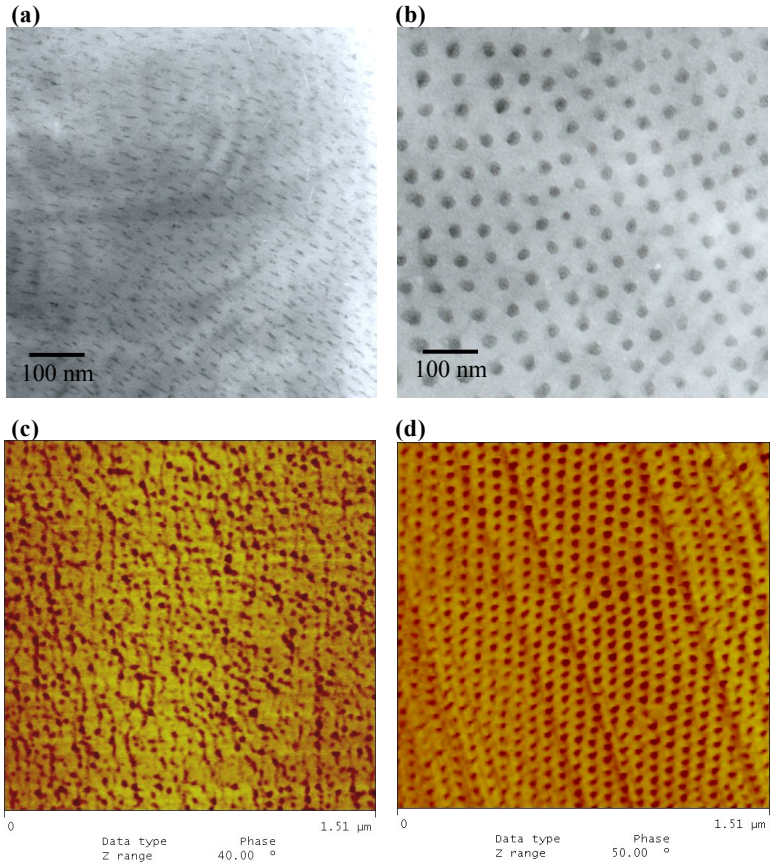

Fig. 2: *(a) TEM image of PS-b-PEO stained by OsO_4. The dark regions correspond to PEO phases stained with OsO_4. (b) TEM image of CdS/PS-b-PEO without staining. (c) AFM images of thin films microtomed from bulk PS-b-PEO and (d) AFM images of thin films microtomed from bulk CdS/PS-b-PEO.*

distribution of mercaptoethanol-modified CdS in the PEO domain is quite possibly due to dipole-dipole interactions between the hydroxyl groups of mercaptoethanol and the PEO block. The diameter of CdS-included PEO spheres is approximately 23 nm and the inter-sphere distance is about 60 nm, as estimated from their TEM images. In order to cover all PEO domains, there must be some distributions of CdS QDs in each PEO domain because the volume fraction of added CdS with respect to the PEO block is about 2.7%, which is not enough to cover each PEO domain fully. It is, however, not possible to detect them with the current techniques.

The results from TEM analysis are consistent with those by SAXS. Further evidence of the two different morphologies can be found in phase-contrast atomic force microscopy images (AFM) of PS-b-PEO and CdS/PS-b-PEO samples, as shown in Figure 2(c) and (d), respectively. A diamond knife used during the microtoming process causes the oblique lines in these figures. The difference in the images of pure PS-b-PEO by TEM and AFM (Fig. 2(a) and 2(c)) could be explained by the fact that the dark PEO domains which appear as inclined short cylinders in bulk can be projected into cylindrical shapes in the transmission electron microscopy study, whereas the topology of the same micro-tomed slice would shows hairy spherical images by the tapping mode of AFM.

Figure 3(a) and (b) shows the wide-angle X-ray diffraction results support the corresponding crystal-to-amorphous change of the PEO domain. In the case of pure PS-b-PEO, two sharp peaks at $2\theta = 19.0^{o}$ and 23.21^{o} represent the crystallinity peaks of the PEO domain after deconvolution, as shown in Figure 5(a). Figure 5(b) shows the decrease of crystallinity of PEO domain when CdS is incorporated into the PEO domain, indicating the change from crystalline to amorphous PEO. This result is also consistent with those obtained by DSC. The possible scenario for this phenomenon is due to the relatively small size of CdS to the contour length of PEO block (2.5nm vs. 130 nm) and the dipole-dipole interaction between the angling hydroxy group of surface-attached mercaptoethanol on CdS and ethylene oxide in PEO domain, CdS are

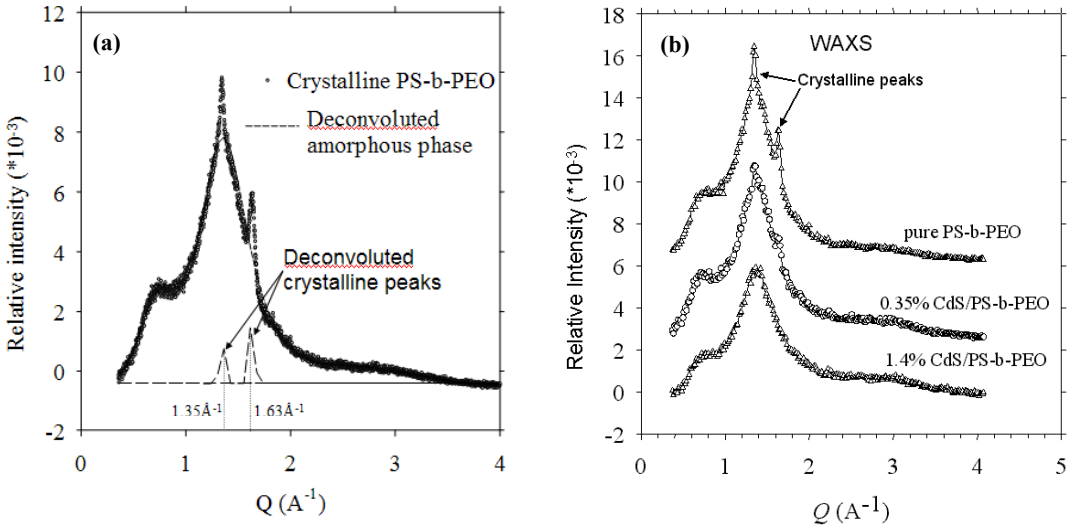

Fig. 3: (a) Deconvolution curves of the WAXS curve of crystallinity PS-b-PEO. (b) WAXS of PS-b-PEO and CdS/PS-b-PEO after crystallization at -20°C for 18 hr.

tethering to PEO chain and appears to destroy the crystallinity of PEO domain, as shown in Scheme 1. This enables CdS-infiltrated PEO domains to be amorphous and to minimize their surface energy by forming either BCC or SC structures.

When only the volume fraction of the block copolymer PS-b-PEO is considered, it is true that in the equilibrium state the pure PS-b-PEO should be in the spherical region with body-center cubic packing due to strong segregation. The morphology of asymmetric amorphous-crystalline block copolymers, however, depends on both the microphase separation of the two blocks and the crystallization kinetics of the crystallizable block. In our study, the hexagonally-packed cylindrical morphology of PS-b-PEO represents a compromise between the microphase separation involving PS and PEO blocks and the crystallization kinetics of the PEO block. The cylindrical morphology of pure PS-b-PEO is in a meta-stable state due to the fast crystallization of the PEO block. The addition of CdS quantum dots into the diblock copolymer inhibits the crystallization of PEO block. The resultant morphology of CdS/PS-b-PEO sample, therefore, is determined largely by the microphase separation involving PS block and CdS/PEO block, (i.e. the crystallization effect is no longer existing).

In conclusion, semiconductor CdS QDs can be selectively dispersed in the PEO domain of PS-b-PEO block copolymer by using a surfactant. The CdS-infiltrated PEO domains are transformed from originally hexagonally-packed cylindrical structures to BCC or SC structures because CdS inhibits the crystallization and minimizes the surface energy of CdS-infiltrated PEO phase. The authors would like to acknowledge the National Science Council for funding this work through NSC 91-2120-M-009-001. Mr. Tsung-Lun Wu is appreciated for his help in experiments and discussions.

BEAMLINE
17B X-ray Scattering beamline

EXPERIMENTAL STATION
X-ray Scattering end station

AUTHORS
S.-W. Yeh and K.-H. Wei
Department of Materials Science and Engineering, National Chiao Tung University, Taiwan

Y.-S. Sun, U.-S. Jeng, and K. S. Liang
National Synchrotron Radiation Research Center, Hsinchu, Taiwan

PUBLICATIONS
- S. W. Yeh, K. H. Wei, Y. S. Sun, U.-S. Jeng, and K. S. Liang, *Macromolecules* **36**, 7903 (2003).
- U.-S. Jeng, Y.-S. Sun, H.-Y. Lee, C.-H. Hsu, K. S. Liang, S.-W. Yeh, and K.-H. Wei, *Macromolecules* **37**, 4617 (2004).
- S. W. Yeh, Y. T. Chang, C. H. Chou, and K. H. Wei, Macromolecular Rapid Communications **25**, 1679 (2004).
- S. W. Yeh, T. L. Wu, and K. H. Wei, Nanotechnology (2004), submitted.
- S. W. Yeh, T. L. Wu, K. H. Wei, Y. S. Sun, and H. S. Liang, J. Polym. Sci. B Polym. Phys. (2004), revised.

CONTACT E-MAIL
khwei@cc.nctu.edu.tw